

# Preparation and isolation of the cellulose nanocrystals from banana leaves by chemical treatments

Dinh Hung Nguyen<sup>1†</sup>, Van Quy Nguyen<sup>1†</sup>, Vinh Tien Nguyen<sup>1</sup>,  
Vu Viet Linh Nguyen<sup>2,\*</sup>

<sup>1</sup>*Faculty of Chemical and Food Technology, Ho Chi Minh City University of Technology and Education, 1 Vo Van Ngan Street, Thu Duc City, Ho Chi Minh, Viet Nam*

<sup>2</sup>*Faculty of Applied Sciences, Ho Chi Minh City University of Technology and Education, 1 Vo Van Ngan Street, Thu Duc City, Ho Chi Minh, Viet Nam*

\*Email: [linhnv@hcmute.edu.vn](mailto:linhnv@hcmute.edu.vn)

Received: 13 August 2023; Accepted for publication: 12 July 2024

**Abstract.** Many banana leaves and other residues from banana trees were discharged as waste annually. This biomass resource could isolate negatively charged and large surface banana cellulose nanocrystals (BA-CNCs). However, very few studies investigate the isolation process and the applications of BA-CNCs. Therefore, in this study, we proposed a procedure for isolating BA-CNCs from banana leaf waste relying on sequential chemical treatments including alkali-, bleaching-, and acid hydrolysis processes, respectively. After each chemical treatment stage, the changes in morphology, size, chemical composition, and crystalline structure of banana fibers were analyzed by scanning electron microscopy (SEM), dynamic light scattering (DLS), Fourier-transform infrared spectroscopy (FT-IR), and X-ray diffraction (XRD) methods, respectively. Noticeably, the SEM images showed that these isolated BA-CNCs had a uniform rod-shaped morphology. The DLS and zeta potential analyses revealed that these CNCs possess an average hydrodynamic size of  $373.1 \pm 48.15$  nm and a surface charge of  $-32.28$  mV, respectively. These nanosized and moderate negative charged CNCs potentiate their applications for various purposes, such as fabrications of composite films, and sorbents for wastewater treatment.

**Keywords:** banana leaves, cellulose nanocrystals, isolation, chemical treatment.

**Classification numbers:** 1.1.1, 2.4.4, 2.5.1

## 1. INTRODUCTION

In recent years, banana leaves or other residues from banana trees, such as stems, pseudostems, and fruit peels, have become a significant source of biomass [1 - 3]. Banana trees appear in many areas across Viet Nam, and the reuse of enormous biomass resources from

---

<sup>#</sup> Dedicated to the 13th Vietnam National Conference of Solid Physics and Materials Science (SPMS 2023). CODE: D-74

<sup>†</sup>These authors contributed equally to this work

bananas has gained tremendous attention from researchers [2]. Some emergent studies exploited banana leave waste [1, 3], banana pseudostems [4, 5], and banana peels [2, 6, 7] then are used in many different applications, such as fuel briquettes [1], biodegradable masks [3], packaging film [5], sorbents for wastewater treatment [6, 7] and food additives [2].

Cellulose is the main component of plant cells in biomass resources, whose structure consists of  $\beta$ -1,4-glucopyranose linkage units. As a functional classification of cellulose, cellulose nanocrystals (CNCs) emerged as a revolutionarily ubiquitous material in the last two decades. In particular, CNCs are made by hydrolyzing the amorphous components and recovering the crystalline portions in the cellulose molecular structure. Owing to the high degree of crystallinity, identical particle diameter, a rather high aspect ratio, large surface area, and negatively charged surface, CNCs are applied in many fields such as composite film fabrication, water purification, wastewater treatment, etc. [4, 6 - 9]. In wastewater treatment, CNCs are used to absorb water pollutants such as heavy metal ions, pigments/dyes, and organic molecules [8, 10, 11]. Many researchers put an enormous effort to synthesize CNCs from various plant sources and characterize their size, quality, and potential applications [4, 10, 12, 13]. However, the studies on CNCs from banana leaves are very few, evoking the exploitation and reuse of this extensive biomass resource. In fact, banana leaf waste contains 21.9 - 32.56 % cellulose, 12 - 25.8 % hemicellulose and 17 - 39.1 % lignin (per dry mass), which could be employed as feedstocks for acquiring various lignocellulosic products including cellulose nanofiber, lignocellulosic micro/nanofiber, bacterial nanocellulose (BNC), and CNC [4, 14]. To eliminate hemicellulose and lignin components during the preparation of cellulose derivatives from banana lignocellulosic by-products, these biomass residues first underwent a pretreatment process, either physical approach, or biological method, or chemical strategy, or the combination of these above-mentioned methods [3, 4, 14]. Particularly, physical approaches were insufficient to completely remove hemicellulose and lignin compositions [3]. Whereas, although biological strategies render environmental sustainability, they face varying challenges such as complicated procedures, high production costs, an additional physical or chemical purification of melanoidin, and dependence on banana leaf quality, involving planting nutrition, and crop management [14]. In this regard, there was a requirement for a mixture of delicate medium (such as fruit juices, or corn liquor) and a symbiotic culture of bacteria and yeast, which is a microbial mixture of yeast, acetic acid bacteria, and lactic acid bacteria to acquire BNC-containing biofilms from tea fungus [14]. Even though the chemical strategy produces a discharged efflux that needs to be passed through treatment before returning to the surrounding environment, it possesses many advantages in terms of cellulose derivatives production, such as low production cost, simple process, high reproducibility, less dependence on the quality of banana leaves [4, 5, 7, 12]. There are still many studies that solely use acid, base, or oxidizing reagents, or a mixture of them during the pretreatment and hydrolysis of banana leaf waste to recover cellulose and fabricate nanocellulose derivatives [4, 5, 7, 12]. However, there was rare literature that reported a comprehensively detailed procedure for isolating cellulose derivatives from banana leaf waste relying on sequential chemical treatments including base, oxidizing reagent, and acid treatment processes, as well as investigating the base-treatment conditions, such as temperature, time, and reagent concentration, and the bleaching and non-cellulosic composition removal abilities between varying oxidizing reagents [4, 5, 7, 12].

In this study, the CNCs were isolated from banana leaf fibers through sequential chemical processes, including alkali, bleaching agents, and sulfuric acid hydrolytic treatments. Importantly, the alkali-treatment conditions, such as temperature, time, and NaOH concentration, as well as the bleaching and non-cellulosic component clearance capabilities between different bleaching agents (hydrogen peroxide, sodium hypochlorite) were investigated to unveil the

effective parameters for the CNC isolation. The morphology, size, surface charge, functional groups, and crystallinity degree properties of the extracted banana fibers were also evaluated.

## 2. MATERIALS AND METHODS

### 2.1. Materials

Areca banana leaves from 12-month-old banana trees were harvested at the farm in Vung Tau City, Ba Ria–Vung Tau province, Viet Nam. Sodium hydroxide (NaOH), hydrogen peroxide ( $\text{H}_2\text{O}_2$ , 30 wt.%), sodium hypochlorite ( $\text{NaClO}$ , 8 wt.%), and sulfuric acid ( $\text{H}_2\text{SO}_4$ , 98 wt.%) were supplied by Xilong Scientific Co., Ltd. (China). Distilled water (DI) was obtained from VN Chemsol Co., Ltd. (Viet Nam). All solvents were of analytical grade and used without purification.

### 2.2. Preparation of microfibrillated cellulose from banana leaves

The non-cellulosic components in banana leaves were eliminated and then CNCs were isolated by chemical treatment based on some reported procedures for natural fibers [4, 12, 13].

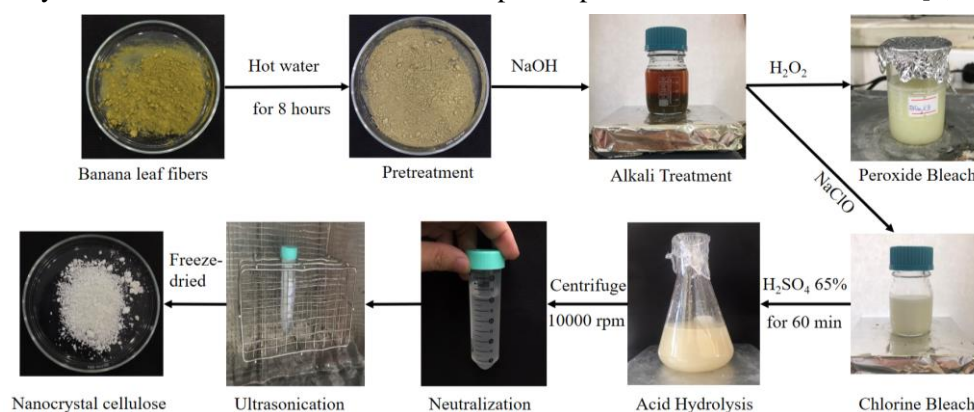


Figure 1. Schematic of the isolation of CNCs from banana leaves.

Table 1. Experimental parameters for chemical treatment of banana leaves.

Sample name	NaOH concentration, C% (wt.%)	Time treatment (hrs)	Temperature (°C)
Na1-60-2	1	2	60
Na1-80-1	1	1	80
Na1-80-2	1	2	80
Na1-80-4	1	4	80
Na1-100-2	1	2	100
Na4-80-2	4	2	80
Na4-80-4	4	4	80
Na8-80-4	8	4	80

Figure 1 illustrates the entire process of preparing microfibrillated celluloses (MFCs) and isolating CNCs from banana leaves. Firstly, dried banana leaves were washed with 100 °C water for 8 hrs to remove dirt and aqueous soluble substances like wax and pectin. Next, the clean banana leaves were dried and, then milled in the ball mill (SD/2–1000, Ceramic Instrument Slr, Sassuolo, Italy) before sieving using sieves with two different sizes (< 310 µm and > 150 µm)

on the auto sieve shaker (A060-01, Controlab, France). Subsequently, 10 g of the samples were treated with different NaOH solution concentrations (1, 2, 4, and 8 wt.%) at varying temperature conditions (60, 80, and 100 °C) for various reaction times (1, 2, and 4 hrs) (Table 1). The samples were bleached twice with 4 wt.% H<sub>2</sub>O<sub>2</sub> solution or with 4 wt.% NaClO solution at 60 °C for 2 hrs.

### 2.3. Isolation of the CNCs from MFCs

The CNCs were continuously isolated from banana MFCs (code BA-CNC) following Figure 1. Briefly, 10 g bleached banana powder was acidified in 65 wt.% H<sub>2</sub>SO<sub>4</sub> solution with the sample: acid solution ratio of 1:30 (g/ml) for different acidification times of 60 min. To terminate the acid hydrolysis reaction, the suspension was then diluted five times with 10 °C cold distilled water. Afterwards, the suspended crystals were washed three times in distilled water by centrifugation at 10000 rpm for 10 min. The crystals were then sonicated in the ultrasonic bath for 60 min. Finally, the samples were freeze-dried at -40 °C to -50 °C for 48 hrs to acquire the resulting BA-CNC.

### 2.4. Characterization

The functional groups of banana leaves, MFCs, and BA-CNCs were identified and analyzed by Fourier–transform infrared (FT–IR) spectrometer (FT/IR–4700, Jasco Inc., Japan). The spectra were recorded in the wave number range of 500 - 4000 cm<sup>-1</sup> under the attenuated total reflection (ATR) mode with a scanning speed of 2 mm/sec at 25 °C. The morphologies of BLF, Na-BLFs, MFCs and BA-CNC were identified by the scanning electron microscopy (SEM) method on Hitachi MiniSEM, and FE-SEM on Hitachi S4800 (Japan). These samples were coated with platinum before the measurements, and an accelerating voltage of 15 kV.

The crystallinity of banana leaves, MFCs and BA-CNCs was characterized using the X-ray diffraction (XRD) method on an X-ray diffractometer (D8 ADVANCE, Bruker, USA). Radial scans of intensity were captured at an ambient condition over a diffraction  $2\theta$  angles from 5° to 40° (step size = 0.02°) using a Ni-filtered Cu K $\alpha$  radiation source ( $\lambda = 1.54 \text{ \AA}$ ), an operating voltage of 45 kV. The crystallinity index (CrI) of each sample was calculated by referring to the diffraction intensity of crystalline and amorphous regions following Segal's empirical equation (1) [14, 15]:

$$\text{CrI (\%)} = \frac{I_{200} - I_{\text{am}}}{I_{200}} \times 100 \quad (1)$$

where  $I_{200}$  is the peak intensity at the (200) plane at a diffraction  $2\theta$  angle of 22.7°,  $I_{\text{am}}$  is the minimum intensity of the uncrystallized region between (200) and (110) lattices ( $2\theta = 18^\circ$ ).

The average crystallite sizes (L) of the isolated cellulose samples were identified using Scherrer's equation (2) [16, 17]:

$$L = \frac{K\lambda}{\beta \cdot \cos \theta} \quad (2)$$

where L is the size of the crystal in nanometers, K is the Scherrer's constant (0.91),  $\lambda$  is the radiation wavelength of X-ray (1.54 Å),  $\beta$  is the full width at half maximum (FWHM) of the diffraction peak at (200) lattice, and  $\theta$  is the angle of diffraction peak (°).

The size and size distribution of the extracted cellulose samples were analyzed using the dynamic light scattering (DLS) method on a Malvern Zetasizer Pro (Malvern Panalytical, UK) at 25 °C. The BA-CNC solution was prepared at a concentration of 0.1 % (w/v).

### 3. RESULTS AND DISCUSSION

#### 3.1. Effect of treatment temperature, time, and NaOH concentration on the banana fibers extracted from banana leaves

Treatment temperature, treatment time, and NaOH concentration will affect the chemical composition of natural fibers [18 - 20]. First, the effect of treatment temperature and then treatment time on the BLFs was investigated following the table 1. Afterwards, the banana fibers will be further examined with different NaOH concentrations (1, 2, 4, and 8 wt.%) under the effective conditions of treatment temperature and time. As shown in Figure 2a, the FT-IR spectra of the untreated and NaOH-treated banana leaf fibers (Na-BLFs) at different temperature conditions showed peaks at 3500 - 3100  $\text{cm}^{-1}$ , 2920  $\text{cm}^{-1}$ , and 2850  $\text{cm}^{-1}$ , which could be attributed to the O-H group, C-H asymmetric and symmetric stretching vibrations in the structure of cellulose and hemicellulose [20]. The characteristic peaks at 1728  $\text{cm}^{-1}$  and 1620  $\text{cm}^{-1}$  assigned to the C=O stretching vibration of acetyl and uronic ester groups of hemicellulose and xylans or ester bonds in carboxylic groups of ferulic and *p*-coumaric acids in lignin, respectively [15, 20]. The intensity of these peaks decreased when the treatment temperature increased from 60 °C to 80 °C; however, it was nearly unchanged when the temperature elevated from 80 °C to 100 °C. This indicates that the relatively high micro-crystalline structure was obtained after the effective alkali treatment at 80 °C and the acceleration of 20 °C is insufficient to remove additional non-cellulosic materials from BLFs. The result indicated that 80 °C is likely the effective temperature for the chemical treatment of BLFs with 1 wt.% NaOH solution for 2 hrs.

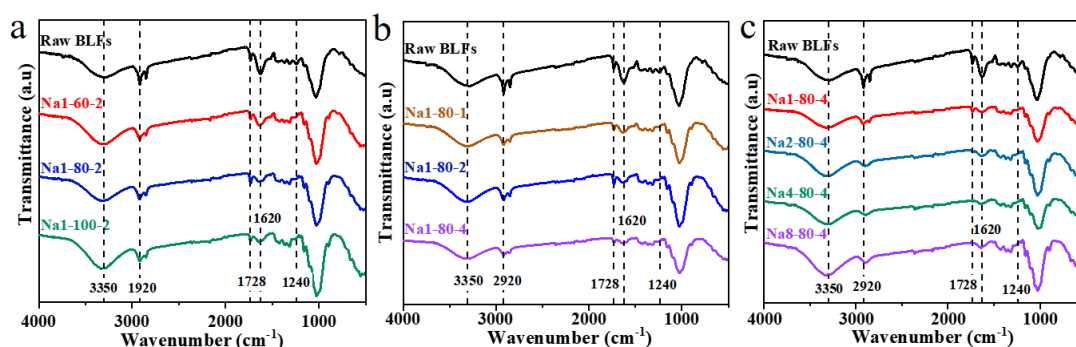


Figure 2. FT-IR spectra of the NaOH-treated banana leaves in different (a) treatment temperatures, (b) treatment times, and (c) NaOH concentrations.

As shown in Figures 2a and 2b, the peak at 1240  $\text{cm}^{-1}$  indicates the unsaturated bonds C=C stretching vibration of the aromatic ring and aryl C-O group in lignin [12, 15]. The peak at 1045  $\text{cm}^{-1}$  corresponds to the C-O-C stretching of the pyranose ring in the structures of cellulose, hemicellulose, and lignin (Figures 2a and 2b) [7, 20]. The intensity of these peaks decreased with the increasing treatment temperature and time. Collectively, the FT-IR results from Figures 2a and 2b disclosed that the NaOH treatment removed lignin and hemicellulose portions, and the highest efficiency of alkali treatment was obtained when the BLFs were treated at 80°C for 4 hrs. Figure 2c showed the FT-IR spectra of the untreated and Na-BLFs in different NaOH concentrations (1, 2, 4, and 8 wt.%). In the spectrum of untreated BLFs, the peaks at 2920  $\text{cm}^{-1}$ , 2850  $\text{cm}^{-1}$ , 1728  $\text{cm}^{-1}$ , and 1240  $\text{cm}^{-1}$  correspond to the C-H asymmetric, symmetric stretching vibrations in the structure of cellulose and hemicellulose, the C=O stretching vibration of acetyl and ester groups of hemicellulose and lignin, and the strains of C=C group in aromatic ring and aryl C-O group in lignin [20, 21]. When the BLFs were treated with the 1 wt.% NaOH solution,



although these characteristic peaks were reduced in their intensities, they were still present in the spectrum. This implies that 1 wt.% NaOH concentration could not completely eliminate hemicellulose and lignin components. By contrast, when increasing the NaOH level up to 2 wt.%, the doublet intense peaks at  $2920\text{ cm}^{-1}$  and  $2850\text{ cm}^{-1}$  become a broad single band ( $2916\text{ cm}^{-1}$ ). Moreover, the peaks at  $1728\text{ cm}^{-1}$  and  $1240\text{ cm}^{-1}$  content nearly disappeared. There were insignificant differences in the spectra of Na2-80-4, Na4-80-4, and Na8-80-4 samples. These observations indicated that NaOH concentration affects the removal of hemicellulose and lignin greater than the treated temperature and time. The FT-IR results in Figure 2 indicate that the highest efficiency of alkali treatment was acquired when the BLFs were treated at 2 wt.% NaOH concentration,  $80\text{ }^{\circ}\text{C}$  for 4 hrs.

### 3.2. Effect of bleaching agents on the MFCs extracted from alkali-treated banana leaves

Two types of bleaching agents, including hydrogen peroxide ( $\text{H}_2\text{O}_2$ ) and sodium hypochlorite ( $\text{NaClO}$ ), were carried out to determine their bleaching and lignin removal effects for NaOH-treated BLFs [22]. After treating with 2 wt.% NaOH at  $80\text{ }^{\circ}\text{C}$  for 4 hrs, the Na-BLFs were treated twice with 4 wt.%  $\text{NaClO}$  solution or 4 wt.%  $\text{H}_2\text{O}_2$  solution at  $60\text{ }^{\circ}\text{C}$  for 2 hrs, code name are ClO-60-2 and  $\text{H}_2\text{O}_2$ -60-2, respectively.

#### 3.2.1. Morphology of the extracted MFCs with different bleaching agents

After each chemical treatment, the macroscopic photos of banana leaf fibers (BLFs) were taken and displayed in Figure 3.

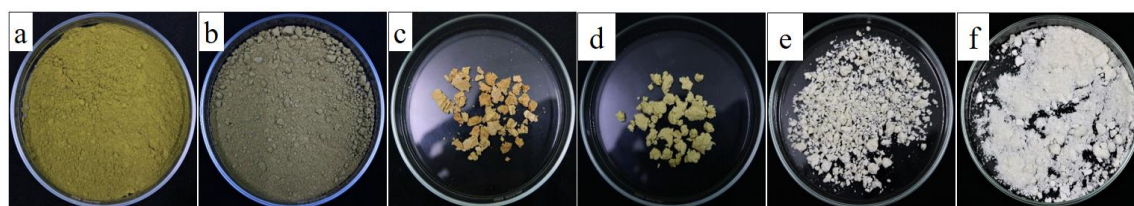


Figure 3. Photographs of (a) raw BLFs, (b) hot water-treated BLFs, (c) Na2-80-4-treated BLFs, (d)  $\text{H}_2\text{O}_2$ -60-2, (e) ClO-60-2 and (f) BA-CNC.

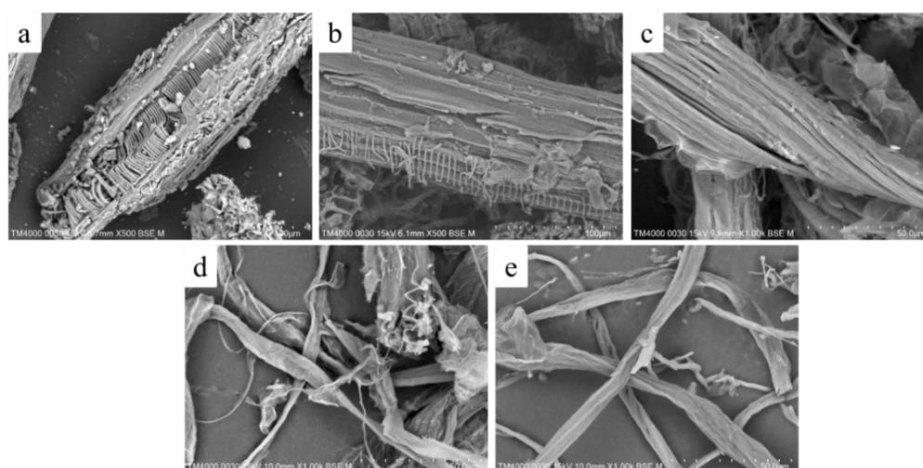


Figure 4. SEM images of (a) raw BLFs, (b) hot water-treated BLFs, (c) Na2-80-4-treated BLFs, (d)  $\text{H}_2\text{O}_2$ -60-2, and (e) ClO-60-2.

It is worth seeing that the pristine BLF color was sequentially varied from brownish yellow to brownish and then to brownish orange following the initial boiling-water pre-treatment for 8 hrs and subsequent 2 wt.% NaOH treatment at 80 °C for 4 hrs (Figures 3a-c). Following the bleaching stage with hydrogen peroxide and sodium hypochlorite at 60 °C for 2 hrs, the colors of BLFs were yellow and greyish-white, respectively (Figures 3d and 3e). The acquired BA-CNC possessed a white color (Figure 3f).

The change in color of these samples could be attributed to the removal of non-cellulosic materials and other impurities, such as hemicellulose, lignin, pectin, and wax, accounting for the darkness of the MFC samples. The morphology of BLFs was further investigated through SEM images (Figure 4). The original BLFs hold a bundle-like shape with a diameter of 80  $\mu\text{m}$ , presumably due to lignin acting as adhering material (Figure 4a). Then hot water-treated BLFs kept the size, but the surface of samples were smoother because of the removal of dust, wax and a small part of lignin on the surface of BLFs (Figure 4b). Subsequently, following the NaOH treatment, the bulky bundles of BLFs diverged into thinner bundles with their diameters ranging from 26.73 to 37.65  $\mu\text{m}$  (Figure 4c). This observation indicated that the alkali treatment partially removed non-cellulosic components and other outermost impurities in the microfibrils. As seen in Figures 4d and 4e, the chlorine agent renders more effective in separating the 30  $\mu\text{m}$ -thick fibril bundles into individual fibers whose diameter is roughly 2.9 - 11.86  $\mu\text{m}$ , compared with that of peroxide chemical (6.8 - 29.2  $\mu\text{m}$ ). This decrease in fibril diameter indicated that most of the linkage and binder components in the fibril structure of the Na-BLFs were eliminated, leading to the individual form of fibers. In addition, the chlorine agent is presumably considered to eliminate and break higher adhesive lignin amount which is an amorphous region of cellulosic banana fibers than that of peroxide, as a consequence of its more robust oxidative capability.

### 3.2.2. FT-IR analysis of the microfibrillated cellulose extracted with different bleaching agents

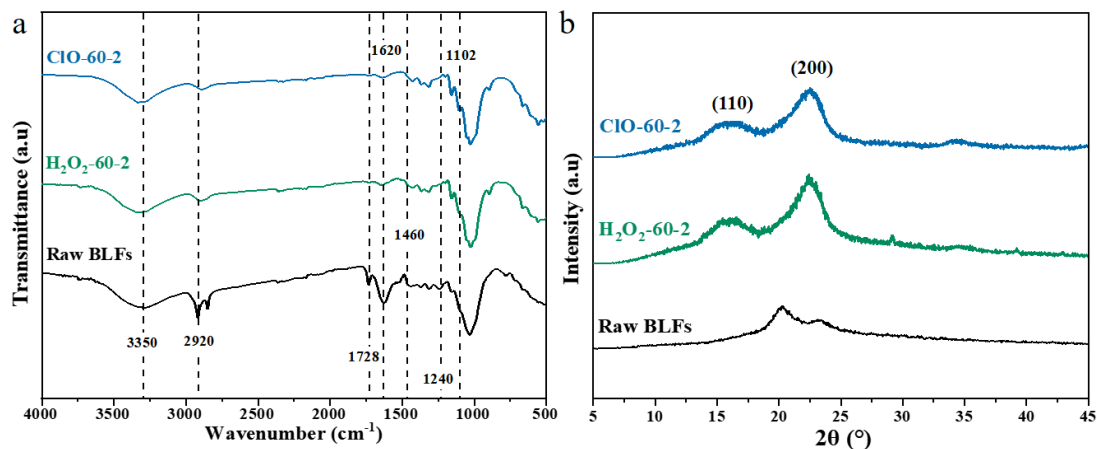


Figure 5. (a) FT-IR spectra and (b) XRD patterns of the raw BLFs, bleached BLFs with different agents.

As shown in Figure 5a, the doublet prominent peaks at 2920 and 2850  $\text{cm}^{-1}$  on the spectrum of raw BLFs, which are ascribed to the C-H groups in cellulose structure, became a broad single band (2916  $\text{cm}^{-1}$ ) on all spectra of treated BLFs. In addition, the characteristic peaks at 1728 and 1620  $\text{cm}^{-1}$  on these spectra, corresponding to the C=O stretching vibration of acetyl and ester groups of hemicellulose and lignin and hydrogen bonding, are significantly reduced after bleaching. Besides, the intensity of emergent peaks at 1460 and 1240  $\text{cm}^{-1}$ , which are assigned to the stretching vibrations of the C=C group on the aromatic ring and aryl C-O group of lignin,

remarkably decreased after alkali treatment and vanished after bleaching with NaClO or H<sub>2</sub>O<sub>2</sub> t, indicating the elimination of most of the lignin portion by these chemicals. Specifically, the typical peaks at 1102 cm<sup>-1</sup>, correlating to the C–O–C stretching of cellulose's pyranose ring, were seen in the spectra of ClO-60-2 samples, implying the highest bleaching efficiency of NaClO treating process. Consequently, the FT-IR results revealed that the highest bleaching efficiency was acquired when the Na-BLFs were treated twice with 4 wt% NaClO solution at 60 °C for 2 hrs.

Figure 5b illustrates the XRD patterns of the raw BLFs and bleached BLFs. A broad diffraction peak and a minor shoulder at  $2\theta$  angles of 21.9° and 22.7° were attributed to the (200) diffraction lattice in the XRD pattern of raw BLFs. The highest intensities ( $I_{200}$ ) of the ClO-60-2 and H<sub>2</sub>O<sub>2</sub>-60-2 samples corresponded to the (200) reflected planes, and were observed at  $2\theta$  angles of 22.7°, while  $I_{am}$  is observed at approximately 19.61°. At  $2\theta$  angles of 16°, the appearance of peaks in the XRD patterns of the bleached BLFs was attributed to the (110) diffraction lattice and it indicates that cellulose structure has been improved [18, 21, 23, 24]. After H<sub>2</sub>O<sub>2</sub> or NaClO treatment, the CrI was risen from 48.43 % (raw BLFs) to 53.58 % and 58.56 % for H<sub>2</sub>O<sub>2</sub>-60-2 and ClO-60-2, respectively. The CrI of raw BLFs is the lowest value because of the presence of lignin, which is an amorphous and adhesive chemical in banana fibers. Whereas, the bleaching process effectively removed the lignin from BLFs so the CrI of the bleached samples increased [4, 12]. In addition, the CrI of the ClO-60-2 sample was higher than H<sub>2</sub>O<sub>2</sub>-60-2 samples nearly 5 %. This indicates that NaClO agent bleached BLFs more significant than H<sub>2</sub>O<sub>2</sub>.

### 3.3. Isolation of the CNCs from MFCs

After determining the effective conditions in the first two treatment stages, the banana MFCs were ultimately treated with H<sub>2</sub>SO<sub>4</sub> solution (65 wt.%) to acquire the resulting banana cellulose nanocrystals (BA-CNCs). These BA-CNCs were sequentially characterized by their morphology (Figure 6a), size, surface charge (Figures 6b and 6c), functional groups (Figure 7a), and crystalline degree (Figure 7b).

#### 3.3.1. Morphology, size, and size distribution analyses of the CNCs

The obtained BA-CNCs were observed in their nanosized structure using FE-SEM analysis (Figure 6a).

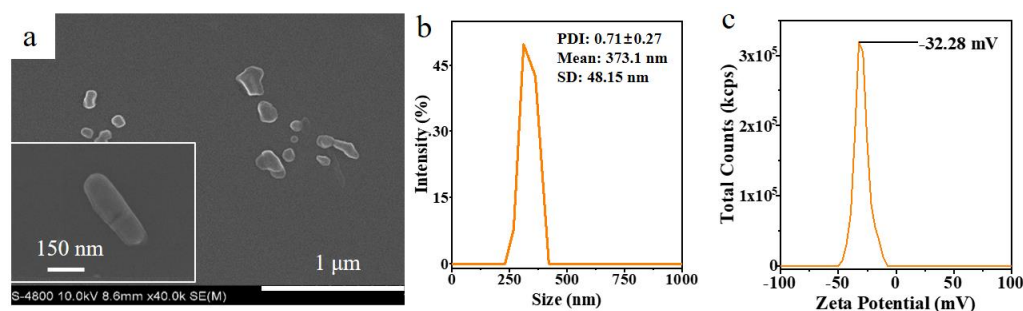


Figure 6. (a) SEM image with  $\times 40,000$  magnification (inset: the  $\times 150,000$  magnification), (b) size distribution, and (c) zeta potential of BA-CNC.

In this regard, most of the BA-CNCs possessed a rod-shaped morphology with mean diameters of 80 nm, lengths of 320 nm, and an aspect ratio of approximately 4. This finding was



explained by the penetration and cleavage of hydronium ions into the amorphous portion of semicrystalline microfibrils during sulfuric acid treatment [4, 12, 13, 24]. Next, through DLS measurement, the BA-CNC had a monomodal size distribution and a narrow distributed region (ranging from 230 to 400 nm) with the size peak at 310 nm, implying the successful nanosized synthesis and uniform size of the acquired BA-CNC. In turn, the average size and polydispersity index (PDI) of the BA-CNC were  $373.1 \pm 48.15$  nm and  $0.71 \pm 0.27$  (Figure 6b). As seen in Figure 6c, the BA-CNC surface possessed a negative charge with an zeta potential of  $-32.28$  mV, due to hydroxyl and sulfate groups after the fiber treatment with sulfuric acid. This zeta potential value drops between  $-20$  to  $-30$  mV, which is classified as moderately stable, reducing the repulsive force between CNC colloids and consequently facilitating the closer distribution of CNCs, resulting in an improved mechanical strength for the CNC-based nanocomposite [4, 12, 13].

### 3.3.2. FT-IR and XRD analyses of the CNCs

Figure 7a shows the FT-IR spectra of raw BLFs and BA-CNC. The bands around  $1600$ – $1620$   $\text{cm}^{-1}$ ,  $1728$ , and  $1240$   $\text{cm}^{-1}$ , which in turn are regarded as the stretching vibrations of aromatic ring's C–C in the lignin, C=O units of lignin and hemicellulose, and C–O–C groups of aromatic ether linkages in lignin, significantly decreased or absent in the spectrum of BA-CNC sample [16]. This finding indicates the clearance of lignin and hemicellulose following the alkali and NaClO bleaching treatments. Besides, the characteristic peaks around  $897$ ,  $1052$ – $1032$ , and  $1161$   $\text{cm}^{-1}$  correspond to stretching vibrations of the C1–H, C–O (from C2, C3, and C6), pyranose ring's C–O–C bonds in the cellulosic material, respectively, are observed in the BA-CNC spectrum [16]. As presented in Figures 5 and 7a, there are no remarkable changes in the spectra of NaClO-treated and hydrolyzed BLFs. This observation implies that the acid hydrolysis did not change the cellulose molecular structure of alkali and NaClO-treated fibers.

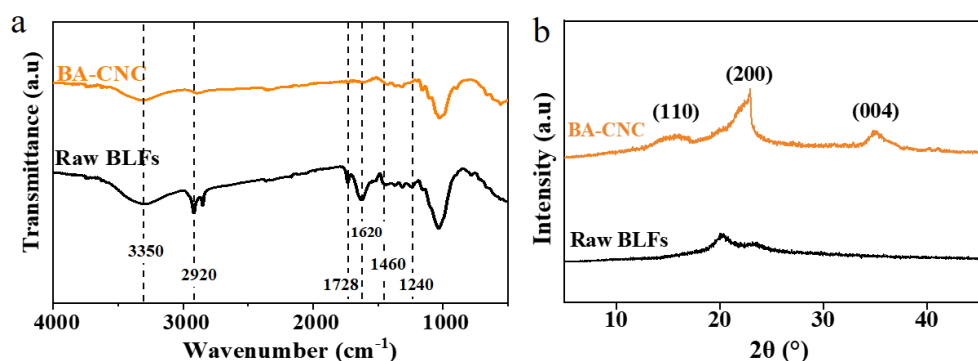


Figure 7. (a) FT-IR spectra and (b) XRD patterns of raw BLFs and BA-CNC.

As shown in Figure 7b, the raw BLFs displayed a broad diffraction peak and a minor shoulder at  $2\theta$  angles of  $21.9^\circ$  and  $22.7^\circ$ , attributed to the (200) diffraction lattice. In the pattern of BA-CNC, the peaks at  $21.9^\circ$  and  $22.7^\circ$ , in turn, were significantly reduced and prominently arose, indicating the increase in the crystalline structure after the chemical treatments. Besides, the BA-CNC pattern also displayed crystalline peaks at  $2\theta$  angles of  $16^\circ$  and  $35^\circ$ , corresponding to the (110) and (004) reflected planes, which are characteristic of type I cellulose structure [16]. In addition, the CrI of raw BLFs and BA-CNC were calculated at 48.43 % and 69.33 %, the crystallite sizes (L) of these samples were also calculated to be 0.44 nm and 1.72 nm respectively following the equation (2), showing that the CrI and the crystallite size of the

samples increased through treatments. These results could be explained by the ultrasonic cavitation-assisted hydrolytic cleavage of glycosidic bridges in amorphous regions of cellulose structure, removal of hemicellulose, lignin, and other non-cellulosic components from the semicrystalline matrix of holocellulose, eventually inducing uniformly scattered crystallites following the sequential chemical treatments [4, 12, 13, 24]. These results agreed with the morphology and FT-IR findings, indicating a compact structure of BA-CNC cellulosic crystallites.

#### 4. CONCLUSION

In this work, banana leaf waste was exploited and reused to produce more useful CNC upon consecutive chemical treatments, including alkali-, bleaching-, and acid hydrolysis stages. Through FT-IR analysis, we observed that the effective alkali and bleaching conditions are 2 wt.% NaOH solution, 80 °C for 4 hrs and NaClO (4 wt.%) at 60 °C for 2 hrs. The macroscopic images, SEM, and FT-IR results revealed that hypochlorite had a greater ability in hemicellulose and lignin removal. After these stages, the BA-CNCs were isolated by treating them with sulfuric acid (65 wt.%). The obtained BA-CNCs presented a uniform rod-shaped morphology with a diameter of 80 nm and length of 320 nm, and an average hydrodynamic diameter of  $373.1 \pm 48.15$  nm and a surface charge of -32.28 mV through SEM, DLS, and zeta potential analyses, respectively. This preparation method exerted a BA-CNC extraction yield of  $24.83 \pm 5.48$  %. In addition, these particles showed a sharp peak at a diffraction angle  $2\theta$  of  $22.7^\circ$  via XRD analysis, indicating the enhanced degree of cellulose crystallinity in this material. These characteristics promise their applicability in various fields, such as fabrications of composite films, adsorbents for heavy metal ions. Nevertheless, quantitatively compositional analysis, such as the contents of cellulose, lignin, hemicellulose, and other non-cellulosic components should be further investigated.

**Acknowledgments.** We acknowledge the support of time and facilities from Ho Chi Minh City University of Technology and Education for this study.

**CRedit authorship contribution statement.** Vu Viet Linh Nguyen: Methodology, Investigation, Supervision, Writing; Dinh Hung Nguyen: Conducting all experiments, Writing; Van Quy Nguyen: Writing, Discussion; Vinh Tien Nguyen: Formal analysis, Discussion.

**Declaration of competing interest.** The authors have no conflict of interests.

#### REFERENCES

1. De Oliveira Maia B. G., Souza O., Marangoni C., Hotza D., De Oliveira A. P. N., Sellin N. - Production and characterization of fuel briquettes from banana leaves waste, *Chem. Eng. Trans.* **37** (2014) 439-444. <https://doi.org/10.3303/CET1437074>
2. Mohd Zaini H., Roslan J., Saallah S., Munsu E., Sulaiman N. S., Pindi W. - Banana peels as a bioactive ingredient and its potential application in the food industry, *J. Funct. Foods* **92** (2022) 105054. <https://doi.org/10.1016/j.jff.2022.105054>
3. Vang H. A., Tran Q. V., Le P. N., Huynh N. A. T., Nguyen V. V. L. - Fabrication of biodegradable masks from banana leaves by thermal compression method, *Version B of Vietnam J. Sci. Technol.* **65** (6) (2023) 31-36. [https://doi.org/10.31276/vjst.65\(6\).31-36](https://doi.org/10.31276/vjst.65(6).31-36)
4. Merais M. S., Khairuddin N., Salehudin M. H., Mobin Siddique M. B., Lepun P., Chuong W. S. - Preparation and Characterization of Cellulose Nanofibers from Banana Pseudostem

- by Acid Hydrolysis: Physico-Chemical and Thermal Properties, *Membranes (Basel)* **12** (5) (2022). <https://doi.org/10.3390/membranes12050451>
5. Srivastava K. R., Singh M. K., Mishra P. K., Srivastava P. - Pretreatment of banana pseudostem fibre for green composite packaging film preparation with polyvinyl alcohol, *J. Polym. Res.* **26** (4) (2019). <https://doi.org/10.1007/s10965-019-1751-3>
  6. Oyewo O. A., Onyango M. S., Wolkersdorfer C. - Application of banana peels nanosorbent for the removal of radioactive minerals from real mine water, *J. Environ. Radioact.* **164** (2016) 369-376. <https://doi.org/10.1016/j.jenvrad.2016.08.014>
  7. Shreedhana K., Ilavarasi R. - Fabrication of nanocrystalline cellulose from banana peel obtained from unripe plantain bananas, *J. Phys. Conf. Ser.* **1644** (1) (2020) 012002. <https://doi.org/10.1088/1742-6596/1644/1/012002>
  8. Tan H. F., Ooi B. S., Leo C. P. (, October 1) - Future perspectives of nanocellulose-based membrane for water treatment, *J. Water Process Eng. Elsevier Ltd.* <https://doi.org/10.1016/j.jwpe.2020.101502>
  9. Goswami R., Mishra A., Bhatt N., Mishra A., Naithani P. - Potential of chitosan/nanocellulose based composite membrane for the removal of heavy metal (chromium ion), In *Mater. Today Proc.*, Elsevier Ltd., Vol. 46, pp. 10954-10959. <https://doi.org/10.1016/j.matpr.2021.02.036>
  10. Voisin H., Bergström L., Liu P., Mathew A. P. - Nanocellulose-based materials for water purification, *Nanomaterials* **7** (3) (2017). <https://doi.org/10.3390/nano7030057>
  11. Thakur V. K., Voicu S. I. - Recent advances in cellulose and chitosan based membranes for water purification: A concise review, *Carbohydr. Polym.* **146** (2016) 148-165. <https://doi.org/10.1016/j.carbpol.2016.03.030>
  12. Mehanny S., Abu-El Magd E. E., Ibrahim M., Farag M., Gil-San-Millan R., Navarro J., ... El-Kashif E. - Extraction and characterization of nanocellulose from three types of palm residues, *J. Mater. Res. Technol.* **10** (2021) 526-537. <https://doi.org/10.1016/j.jmrt.2020.12.027>
  13. Chawalitsakunchai W., Dittanet P., Loykulnunt S., Tanpichai S., Prapainainar P. - Extraction of nanocellulose from pineapple leaves by acid-hydrolysis and pressurized acid hydrolysis for reinforcement in natural rubber composites, In: *IOP Conf. Ser. Mater. Sci. Eng.*, Institute of Physics Publishing, Vol. 526. <https://doi.org/10.1088/1757-899X/526/1/012019>
  14. Nam S., French A. D., Condon B. D., Concha M. - Segal crystallinity index revisited by the simulation of X-ray diffraction patterns of cotton cellulose I $\beta$  and cellulose II, *Carbohydr. Polym.* **135** (2016) 1-9. <https://doi.org/10.1016/j.carbpol.2015.08.035>
  15. Meng F., Wang G., Du X., Wang Z., Xu S., Zhang Y. - Extraction and characterization of cellulose nanofibers and nanocrystals from liquefied banana pseudo-stem residue, *Compos. Part B Eng.* **160** (2019) 341-347. <https://doi.org/10.1016/j.compositesb.2018.08.048>
  16. Mehanny S., Abu-El Magd E. E., Ibrahim M., Farag M., G.S.Millan R., Navarro J., El-Kashif E. - Extraction and characterization of nanocellulose from three types of palm residues, *J. Mater. Res. Technol.* **10** (2021) 526-537. <https://doi.org/10.1016/j.jmrt.2020.12.027>
  17. Flauzino Neto W. P., Silvério H. A., Dantas N. O., Pasquini D. - Extraction and characterization of cellulose nanocrystals from agro-industrial residue – Soy hulls, *Ind.*

- Crops Prod. **42** (1) (2013) 480-488. <https://doi.org/10.1016/j.indcrop.2012.06.041>
18. Parre A., Karthikeyan B., Balaji A., Udhayasankar R. - Investigation of chemical, thermal and morphological properties of untreated and NaOH treated banana fiber, In Mater. Today Proc., Elsevier Ltd., Vol. 22, pp. 347-352. <https://doi.org/10.1016/j.matpr.2019.06.655>
  19. Mustikaningrum M., Cahyono R. B., Yuliansyah A. T. - Effect of NaOH Concentration in Alkaline Treatment Process for Producing Nano Crystal Cellulose-Based Biosorbent for Methylene Blue, IOP Conf. Ser. Mater. Sci. Eng. **1053** (1) (2021) 012005. <https://doi.org/10.1088/1757-899X/1053/1/012005>
  20. Nguyen V. V. L. - Effects of the chemical treatment process with different agents on the morphology and properties of banana fibres, Version B of Vietnam J. Sci. Technol. **65** (1) (2023) 44-48. [https://doi.org/10.31276/VJST.65\(1\).44-48](https://doi.org/10.31276/VJST.65(1).44-48)
  21. Monteiro S. N., Margem F. M., Loiola R. L., de Assis F. S., Oliveira M. P. - Characterization of Banana Fibers Functional Groups by Infrared Spectroscopy, Mater. Sci. Forum **775-776** (2014) 250-254. <https://doi.org/10.4028/www.scientific.net/MSF.775-776.250>
  22. Bajpai P. - Pulp Bleaching, In Biermann's Handb. Pulp Pap., Elsevier, pp. 465-491. <https://doi.org/10.1016/b978-0-12-814240-0.00019-7>
  23. Guimarães J. L., Frollini E., da Silva C. G., Wypych F., Satyanarayana K. G. - Characterization of banana, sugarcane bagasse and sponge gourd fibers of Brazil, Ind. Crops Prod. **30** (3) (2009) 407-415. <https://doi.org/10.1016/j.indcrop.2009.07.013>
  24. Gupta M. K. S. U., S. H. - A facile approach for isolation of cellulose nanocrystals from banana fibres, Indian J. Fibre Text. Res. **48** (2) (2023). <https://doi.org/10.56042/ijftr.v48i2.64801>